OPTICAL OBSERVATION OF SPACE DEBRIS IN THE GEOSTATIONARY RING

T. Schildknecht[(1)], R. Musci[(1)], M. Ploner[(1)], S. Preisig[(1)], J. de Leon Cruz[(2)], H. Krag[(3)]

[(1)] Astronomical Institute, University of Bern, Sidlerstrasse 5, CH-3012 Bern, Switzerland
Email: thomas.schildknecht@aiub.unibe.ch
Email: reto.musci@aiub.unibe.ch
Email: martin.ploner@aiub.unibe.ch
Email: stefan.preisig@aiub.unibe.ch

[(2)] Instituto de Astrofisica de Canarias, 38200 La Laguna, Tenerife, España
Email: jmlc@ot.iac.es

[(3)] Institute for Flight Mechanics and Space Flight Technology, TU Braunschweig, Hans-Sommer-Str. 5, 38106 Braunschweig, Germany
Email: hkrag@tu-bs.de

ABSTRACT

Currently, the GEO population of debris objects with sizes smaller than 1 m^2 – about the limit of the US Space Command catalogue – is vastly unknown. There is even evidence for an incompleteness of the catalogue at larger sizes. In view of this situation, several space agencies started to perform optical observations of the geostationary ring. NASA conducts optical surveys with a 0.32 m Schmidt telescope equipped with a CCD detector. The European Space Agency (ESA) has also initiated its own program for optical observations of space debris using a 1 m Ritchey-Chrétien telescope on Tenerife (Canary Islands). The efforts have been complemented by an initiative of the Inter-Agency Space Debris Coordination Committee (IADC).

The paper presents the results from the ESA program. Most remarkable is the detection of a previously suspected substantial population of small objects. The survey sampled a limited volume of the orbital element-magnitude space only. In order to asses the observational selection effects the observations have been simulated using a reference population and the ESA PROOF tool.

1. INTRODUCTION

The Geostationary Earth Orbit (GEO) is one of the most valuable regions for telecommunication, Earth observation and space science. Knowing the current debris population in this region is crucial to understand its future evolution and to implement mitigation measures to preserve this environment. The GEO region is especially fragile due to the extremely long lifetimes of debris at this altitude.

Current catalogues and models show a much lower spatial density of small objects in the GEO region than in most LEO altitudes. The limiting object size for the catalogues is about 1 m. For smaller objects we therefore must rely on models. The MASTER model predicts less than 100 fragments in the size range from 0.1 to 1 m [1]. This may be explained by the fact that only two explosions are known to have occurred in GEO (a breakup of an Ekran spacecraft in 1978 and an explosion of a Titan rocket upper stage in 1992). Given this very limited information we may ask if the models reflect the real GEO environment or rather the missing input from observations.

2. THE ESA SPACE DEBRIS TELESCOPE

The ESA Space Debris Telescope is installed in the Optical Ground Station (OGS) at the Teide Observatory

Proceedings of the 3rd European Conference on Space Debris, ESOC, Darmstadt, Germany, 19 - 21 March 2001
(ESA SP-473, August 2001)

on Tenerife, Canary Islands. The OGS serves for the in-orbit checkout of the optical communication payload of the Artemis spacecraft. The ESA Space Debris Telescope is a classical astronomical telescope with a 1 m primary mirror and an English mount. For the debris observations we use the modified Richey-Crétien focus which is equipped with CCD camera. The focal plane array consists of a mosaic of four 2k x 2k pixel CCDs. The total field of view is about 0.7 x 0.7 square degrees and the pixel size is 0.6 arcseconds.

3. THE ESA GEO SURVEY

3.1. Apparent Spatial Density of Catalogue Objects in GEO

Due to natural perturbations the orbital planes of GEO objects have a very specific distribution. The orbital planes of uncontrolled objects exhibit precession motions, which manifests themselves in cyclic variations of the inclinations between 0 and 15 degrees with a period of about 53 years. These precession motions are also responsible for a correlation between the inclinations and the right ascensions of the ascending nodes. Fig. 1 shows the apparent density of the catalogued GEO objects in the right ascension-declination-space, i.e. as seen in front of the stellar background (the small squares mark survey fields and the dark ellipse indicates the Earth shadow, see below).

Fig. 1. Apparent density of the catalogued GEO objects

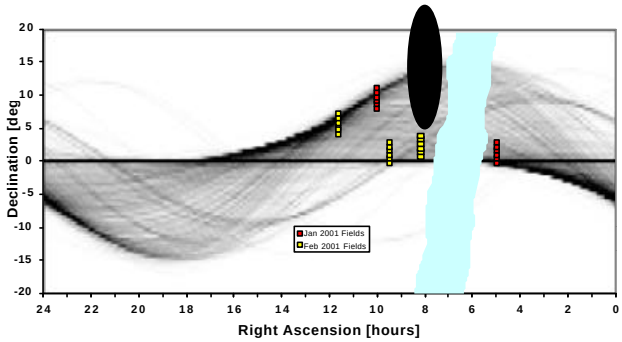

in the right ascension-declination-space (the small squares mark survey fields and the dark ellipse indicates the Earth shadow, see text).

3.2. Observations

The observation scenarios for the January and February 2001 campaigns where chosen to optimize the coverage for certain bands of orbital inclinations while still satisfying observational constraints. With first priority we tried to observe near the Earth's shadow cone in order to optimize the illumination conditions for the objects of interest. During January, however, we also had to avoid the Milky Way, which covered a good part of the evening sky just west of the shadow region. The fields were furthermore placed at the densest region of the catalogue population. In order to increase the probability to re-observe the same objects during several consecutive nights the same sequence of fields was imaged at the same local times during all the nights. Fig. 1 shows the search fields for the two months in the right ascension-declination-space (the small squares roughly correspond to the field of view of the CCD camera). The underlying plot indicates the apparent spatial density of the catalogue population. The Earth shadow region is plotted for January 21, and the light band between 6 and 8 hours right ascension indicates the Milky Way.

The detection technique is based on an algorithm comparing several consecutive frames of the same field in the sky. Fixed background stars are identified on a series of 10 to 30 frames, and the remaining parts of the frames are scanned for any additional objects. During the exposures the telescope is staring into an Earth fixed direction, i.e. is not tracking the sky but potential geostationary objects. After each exposure the telescope has to be repositioned so that the same area of the sky is passing the field of view at the next exposure. The frames are usually exposed for 2 seconds, which is a compromise between a high signal to noise ratio for the objects (long exposures) and a reasonable length for the star trails (short exposure). The exposure repetition rate for a particular field in the sky was set to one per minute meaning that any geosynchronous object detected would be visible on three consecutive frames. Given the current maximum frame repetition rate of about one per 30 seconds (including the repositioning of the telescope) we are able to observe two adjacent fields in parallel.

3.3. Data Reduction

All data was processed in quasi-real-time at the observatory (the results are available about 30 minutes after the observations). The processing is done in batches of about 30 consecutive frames of the same sky field.

The detection procedure is based on a 'masking technique'. The mask is generated from a median frame of the series and thus contains all objects that did not move during the entire series. It particularly contains all background stars. This mask is then applied to each individual frame and the unmasked parts scanned for objects. A filter marks cosmic ray events by virtue of the shape of their intensity profile.

The objects detected at the level of single frames are then correlated and moving objects discriminated according to the expected minimum and maximum apparent motion. For all moving objects their astrometric positions on the individual frames are determined using catalogue stars as a reference. The accuracy of these

positions depends on the magnitude and the apparent motion of the objects, but it is well below one arcsecond even for the faintest objects. Finally a circular orbit is determined for each object (the short arc spanning a few minutes only does not allow to estimate an eccentric orbit).

The correlation with a TLE reference catalogue is done by comparing the observed position with the predicted position as well as by comparing the orbital elements. We thus obtained a list of objects including the determined elements and the TLE data for the correlating objects and a set of small subframes for each detection. The subframes may be used later to manually screen the results. At this stage the uncorrelated ('unknown') objects are named at the level of the mentioned series (i.e. processing batches). A correlation of the unknown objects among the night or even among different nights is done off-line only.

4. RESULTS

Table 1 gives an overview of the ESA GEO campaigns until March 2001. The table includes the 1999 test campaign, which consisted in fact of a first, very limited series of system tests [3]. By 'unknown detections' we denote the detection of a uncatalogued object within a single 30 minute observation series. Some of these detections may actually refer to the same object, i.e. we may have incidentally re-observed some of the objects during the campaign. We use the term 'unknown objects' for uncatalogued objects after having correlated all detections from the campaign. This latter task is in fact identical with creation maintenance of a temporary catalogue of orbital elements for the unknown objects. Currently only the data from the January 2001 campaign have been postprocessed.

Table 1. ESA GEO Campaigns

	Aug/Sept 1999	Jan 2001	Feb 2001
Frames	5'400	15'500	11'300
Scanned Area	895 deg^2	2745 deg^2	2010 deg^2
Obs. Time	13 nights / 49 h	18 nights / 129 h	12 nights / 95 h
Image Data	52 GB	120 GB	86 GB
Unknown detections		**316**	**?**
Unknown objects	**150**	**?**	**?**

Due to the small field of view of 0.7 degrees it is almost prohibitive to perform a complete survey. Fig. 1 gives an impression of the sparse sampling of the orbital element space for the January and February 2001 campaigns. A corresponding diagram showing the January search fields in the horizon system is given in Fig. 2. The observations are obviously limited to small specific regions of the orbital element space. When trying to learn something about the real environment we must be aware of the potentially strong selectional biases of the observation data. We therefore tried to compare the observations with the known catalogue populations as well as with MASTER model [1]. For both cases we used the PROOF (Program for Radar and Optical Observation Forecasting; [2]) tool. PROOF includes a sophisticated model for optical observations and allows predicting detections for a particular observation scenario. To simulate the detections of the catalogued objects we used PROOF in its so-called deterministic mode on the basis of real TLEs. The simulations using the MASTER model did not predict a single uncatalogued object larger than 10 centimeters for the entire January 2001 campaign! This is a clear evidence that MASTER is underpredicting the population for object sizes larger than 10 centimeters by far.

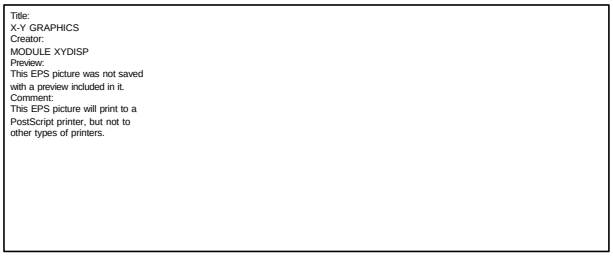

Fig. 2. January 2001 search fields. The dotted line represents the celestial equator.

4.1. Absolute Magnitude Distribution

Fig. 3 shows the magnitude distribution of all detections from the January 2001 campaign. The solid line indicates the instrument sensitivity as determined from independent calibration measurements. All magnitudes have been reduced from apparent magnitudes to so-called absolute magnitudes by correcting for the illumination phase angle. For the scattering properties we assumed a simple Lambert sphere. No reduction to a common distance has been done because of the uncertainties of the determined orbits (see below). The value of this correction would be less than 0.5 magnitudes in most cases. The magnitudes are astronomical 'V magnitudes' and have an accuracy of a few 0.1 magnitudes except at the very faint end where errors could amount to 0.5 – 1 magnitude. The indicated object sizes were derived by assuming Lambert spheres and a bond albedo of 0.1. Both assumptions, however, are uncertain, as long as we don't know the nature of the observed objects.

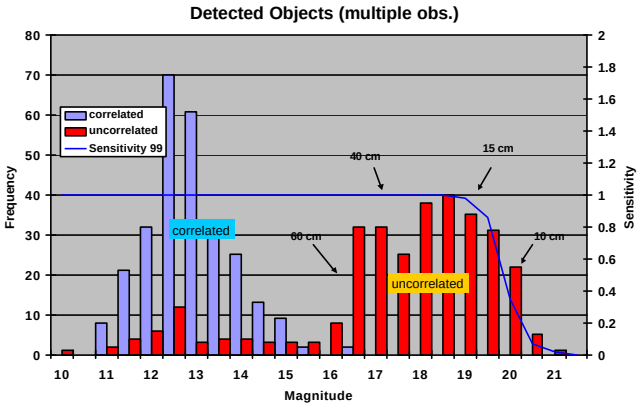

Fig. 3. Absolute magnitude distribution for the detections of the January 2001 campaign.

The distribution is bimodal with the correlated objects clustered around magnitude 12.5, and a large number of uncorreleated objects in the range from magnitude 15 to 21. There are a few bright objects that did not correlate with the available catalogue, most likely due to poor quality of the corresponding elements in the catalogue (e.g. objects that had recently been maneuvered). In addition, some objects were not contained in the reference catalogue. It is important to note that the decrease in number of objects fainter than about magnitude 18 is due entirely to the sensitivity limit of the observation system. The real luminosity function beyond magnitude 18 could therefore still increase! Furthermore we should refrain from directly comparing the number of uncorrelated with the number of correlated objects. Selection effects crucially affect this ratio, e.g. it is strongly depending on the declination of the search fields (results from search fields at the equator are strongly biased towards the controlled, i.e. catalogued objects).

4.2. Inclination Distribution

The inclination distribution is shown in Fig. 4. The bars labeled 'predicted TLE' refer to the detections predicted by PROOF using the catalogue TLEs. In general the distribution of the correlated objects is nicely following the PROOF predictions. However, PROOF is also predicting about 20% more objects than observed. This is explained by several reasons: a) the detection algorithm requires the object to be detected on two consecutive frames whereas PROOF is counting objects appearing on a single frame only, and b) some bright objects may not have correlated due considerable errors in the TLEs.

On the other hand, the distribution of the uncorrelated detections differs significantly from the TLE distribution. There were no uncorrelated objects seen at 0 degree inclination but clear excesses around 13 and around 14 degrees inclination.

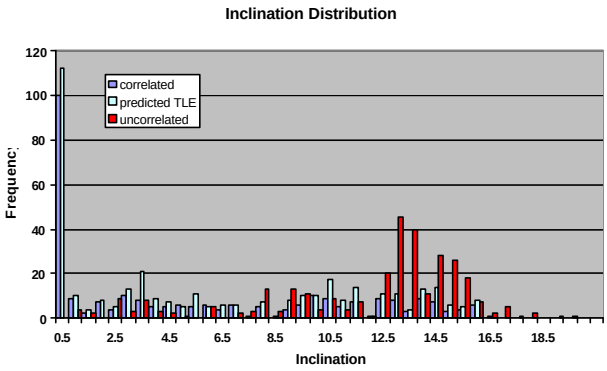

Fig. 4. Inclination distribution for the detections of the January 2001 campaign.

A comparison of the inferred inclinations of the known objects with the corresponding TLE values resulted in a mean error of 0.01 degrees, with a standard deviation of 0.05 degrees. The standard deviation for the positions is 0.15 degrees and is entirely due to the catalogue. We expect larger errors for the inclinations if the comparatively fainter uncorrelated objects, but the effect has not yet been analyzed.

4.3. Distribution Semimajor Axes

The distribution of the semimajor axes is given in Fig. 5. The inferred semimajor axes of the correlated detections are strongly concentrated around the nominal GEO altitude. On the other hand, the uncorrelated detections also have the peak of their inferred semimajor axes at GEO altitude but they are much more dispersed with a slight asymmetry. All semimajor axes were determined assuming circular orbits, which is certainly not true for all objects. Fixing the eccentricity at a wrong value may result in a large error of the inferred semimajor axis. The distribution given in Fig.5 may thus be–depending on the distribution of the true eccentricities–quite meaningless.

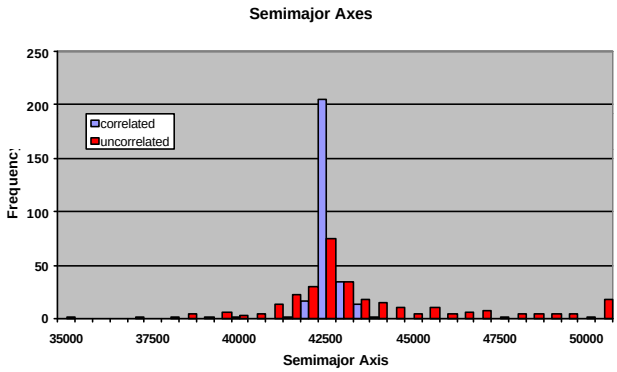

Fig. 5. Semimajor axes of the detections of the January 2001 campaign.

4.4. Inclination and Right Ascension of Ascending Node

The inclination and the right ascension of the ascending node are strongly correlated for the TLE population as we have seen in section 3.1. Fig 7 gives both elements for all correlated and uncorrelated detections. The distinct figure outlined by the correlated objects (black diamonds) is due to the explained 52-year precession period of the orbital planes. Assuming that the objects started at 0 degree inclination the position in the diagram is indicating the age since the end of active inclination control. The objects start at low inclination and at right ascension of the ascending node of about 100 degrees and the gradually evolve to higher inclinations and lower right ascension of the node until they reach the maximum inclination of 15 degrees after 26 years. The oldest catalogue objects have passed this point already.

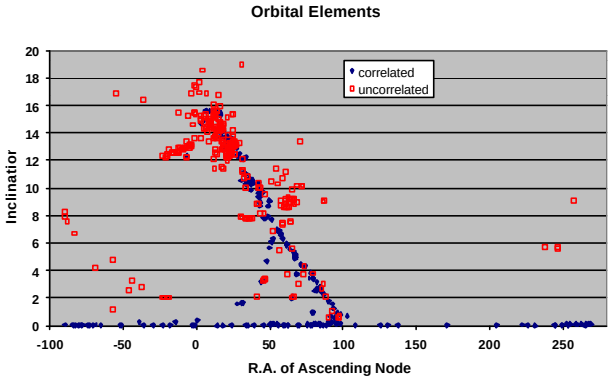

Fig. 6. Inclination versus right ascension of ascending node for all detections of the January 2001 campaign.

The uncorrelated detections (open squares) seem to follow this general evolutionary pattern but they form some striking clusters. The groupings at 8, 9, 13, and 14.5 degrees inclination already showed an enhancement in the inclination distribution compared to the catalogue population. The fact that there are corresponding groupings in right ascension means that these objects in the clusters have common dynamical characteristics. We have checked the clusters for multiple sightings of the same objects and conclude that they are real–a pure selection effect can be excluded on the basis of the arguments given in section 4.2. This data shows for the first time a clear signature of 'clouds' of faint objects confirming the suspected 'clouds' in the 1999 test campaign data.

5. CONCLUSIONS

Current catalogues and models show a much lower spatial density of small objects in the GEO region than in most LEO altitudes. Only two explosions are known to have occurred in GEO and the MASTER predicts less than 100 fragments in size the range from 0.1 to 1 m. The limiting object size for the catalogues is about 1 m.

First results from the ESA GEO survey show a significant, hitherto unknown population of objects in the 0.1 to 1 m size range in the geostationary ring. The observed luminosity function is steadily rising towards smaller sizes up to the observational limit of about 15 cm. For the first time a clear signature of 'clouds' of faint objects has been found. The only plausible source for this debris is breakups of spacecraft, apogee boost motors and rocket upper stages. Due to the small field of view of the ESA telescope the survey is still very inhomogeneous and observational selection effects must be carefully taken into account when using the data to improve debris models.

6. ACKNOWLEDGEMENTS

This work was done under ESA/ESOC contract 11914/96/D/IM. We thank Jyri Kuusela (ESOC) for the technical on-site support at OGS.

7. REFERENCES

1. Bendisch J., Bunte K. D., Krag H., Sdunnus H., Walker R., Wegener P., Wiedemann C., *"Upgrade of the ESA MASTER Model"*, Final report 12318/97/D/IM, Braunschweig, Germany, May 2000

2. Bendisch J., Krag H., Rosebrock J., Schildknecht T., Sdunnus H., Rex D., *Extension of ESA's MASTER Model to Predict Debris Detections*, Final report 12569/D/IM, Braunschweig, Germany, May 2000

3. Schildknecht T., Ploner M. and Hugentobler U., *The Search for Debris in GEO*, 33rd COSPAR Scientific Assembly, July 16 – 23, 2000, Warsaw, Poland, to be published in Advances in Space Research